

Optimizing fiber orientation in fiber-reinforced materials using efficient upscaling

Stefan Frei ^{*} Heiko Andrä [†] Rene Pinnau [‡] Oliver Tse [‡]

Preprint, August 2013

Abstract

We present an efficient algorithm to find an optimal fiber orientation in composite materials. Within a two-scale setting fiber orientation is regarded as a function in space on the macrolevel. The optimization problem is formulated within a function space setting which makes the imposition of smoothness requirements straightforward and allows for rather general convex objective functionals. We show the existence of a global optimum in the Sobolev space $H^1(\Omega)$. The algorithm we use is a one level optimization algorithm which optimizes with respect to the fiber orientation directly. The costly solve of a big number of microlevel problems is avoided using coordinate transformation formulas. We use an adjoint-based gradient type algorithm, but generalizations to higher-order schemes are straightforward. The algorithm is tested for a prototypical numerical example and its behaviour with respect to mesh independence and dependence on the regularization parameter is studied.

1 Introduction

Steadily growing industrial demands on modern materials, such as high stiffness together with minimal weight have led to an increasing interest in composite materials. Combination of different materials yields properties that may differ significantly from the properties of the pure materials. Fiber-reinforced polymers consisting of fibers included in a polymer matrix are used widely in engineering applications, including e.g. aerodynamics or the automotive industry. These materials often show an anisotropic behaviour which highly depends on local concentration and orientation of the fibers inside the matrix (cf. ^[33], ^[1], ^[18], ^[30]). Using modern technology like the fiber-patch-preforming technique ^[20] it is nowadays possible to place fiber bundles quite exactly with nearly every desired orientation within the matrix material. Our purpose is to design an optimal fiber-reinforced material in order to minimize a given objective functional. Our design variable is the local fiber orientation. We assume elastic behaviour for the fiber and the matrix material, respectively, and focus on relatively small deformations such that the linear elasticity equations hold. Further, we assume scale separation (the scale for the fibers is typically in a range of micrometers, while the material we want to study has a scale of millimeters to meters) and use multiscale theory in order to upscale microscopical properties to the macrolevel (^[26], ^[9], ^[25]). For simplicity, we allow only locally unidirectional fibers on the microlevel. Thus, the effective

^{*}Institute of Applied Mathematics, Heidelberg University, Im Neuenheimer Feld 293, 69120 Heidelberg, Germany (stefan.frei@iwr.uni-heidelberg.de)

[†]Fraunhofer Institute for Industrial Mathematics, Fraunhofer-Platz 1, 67663 Kaiserslautern, Germany (heiko.andrae@itwm.fraunhofer.de)

[‡]Department of Mathematics, University of Kaiserslautern, 67663 Kaiserslautern, Germany (pinnau@mathematik.uni-kl.de, tse@mathematik.uni-kl.de)

stiffness tensor will be a function on the macrolevel that in each macroscopic point depends on the local fiber orientation of the underlying microlevel. Clearly, this will only be a reasonable approach if we impose certain smoothness requirements on the macrolevel.

A lot of effort has been spent in literature for the design of optimal microstructures with respect to minimizing compliance, i.e., minimizing complementary energy. For an overview on the topic, we refer to the textbooks of Bendsøe and Sigmund^[7] and Allaire^[2] and the references cited therein. For the case of an orthotropic material the so-called coaxility condition has been derived by different authors, starting from Seregin and Troitskii in^[29]. It states that in the optimal state stress and strain have to share common principal axes, which means that fibers should be aligned with these directions. Many results have been published for cases where an optimal tensor can be derived analytically, e.g. via closed-form formulations of optimality conditions (see e.g.^[27]) or using Hashin-Shtrikman bounds^[15]. These methods have been well-tested for simple geometries, are however restricted to the compliance as objective functional. A numerical approach based on homogenization theory has first been proposed by Bendsøe and Kikuchi in^[8]. Since then, a variety of algorithms have been studied^[3], including two-step optimization algorithms using inverse homogenization (e.g.^[34],^[28]) or stress-based approaches which make use of the coaxility condition^[11]. In both approaches, in each macroscopic integration point a local optimization problem has to be solved each being typically a quite expensive problem for itself in terms of computational cost. This drawback can be circumvented using the Discrete Material Optimization Method (DMO) introduced by Stegmann and Lund^[31],^[32]. Recent results are even available for stochastic loads^[13].

Here, fiber angles are restricted to a finite set of angles for which effective tensors can be computed in advance. While this is the natural framework for material optimization problems, i.e. choosing out of a finite set of materials, fiber angles might in principle take every possible value between 0 and 180 degrees. Furthermore, for practical purposes one might be interested in a smooth behaviour of fiber orientation, for example allowing only slight changes in a neighborhood of a point x .

In order to be able to deal with different kinds of smoothness requirements we approach the optimization problem via a function space setting regarding the fiber angle distribution as a function of space. Our approach allows for rather general objective functionals. The algorithm we propose is a one-level-optimization which optimizes with respect to the design parameters directly. The calculation of effective stiffness tensors is hereby replaced by using coordinate transformation formulas. In this way, it is sufficient to perform one microlevel calculation in advance to calculate one effective tensor for an appropriate reference configuration. During the algorithm no further microlevel calculations are required.

Finally, we end up with an optimal control problem on the macrolevel which is governed by a semilinear state equation. We refer to the textbook of Tröltzsch^[35] and the references cited therein for an overview of known results in this field. Existence and non-existence of solutions for inverse problems have been studied in^[23]. To ensure the well-posedness in our case we include a Tikhonov regularization in the objective functional. In this way we can also control the smoothness of the fiber orientation function α .

1.1 The Optimal Control Problem

In three dimensions the local orientation in a point $x \in \Omega$ can be prescribed by two angles $\alpha_1(x), \alpha_2(x)$, e.g., α_1 prescribing the orientation within the x-y-plane which means perpendicular to the z-axis, α_2 the orientation perpendicular to the x-axis. In this article, we keep α_2 constant, for simplicity, and focus on rotations within the x-y-plane ($\alpha = \alpha_1$). Generalization to optimizing α_1 and α_2 , respectively, is straightforward. We want to solve the following optimization problem

given a convex functional J^u , a body force f , boundary forces g and boundary displacements u^d .

$$\begin{aligned} \min_{(\alpha, u) \in \mathcal{Q}^{\text{ad}} \times \mathcal{U}} J(\alpha, u) &:= J^u(u) + \frac{\kappa}{2} \|\alpha\|_{\mathcal{Q}}^2 \\ \text{subject to} \quad & -\operatorname{div} \sigma = f \quad \text{in } \Omega, \\ & \sigma = A(\alpha)e(u) \quad \text{in } \Omega, \\ & u = u^d \quad \text{on } \Gamma \\ & \sigma \cdot n = g \quad \text{on } \partial\Omega \setminus \Gamma, \end{aligned}$$

where Γ denotes the Dirichlet part of the boundary $\partial\Omega$ of the bounded domain $\Omega \subset \mathbb{R}^3$ and n is the outward unit normal along $\partial\Omega$. The spaces \mathcal{U} and \mathcal{Q} as well as the set of admissible design variables $\alpha \in \mathcal{Q}^{\text{ad}} \subset \mathcal{Q}$ will be defined in the following sections.

Besides compliance the objective functional J^u might as well be the minimization of certain deformation or stress components or arise from inverse problems (deformation or stress tracking). As for practical purposes a smooth behaviour of the fiber orientations is desirable, we choose an H^1 -regularization for our work.

For the discretization we use the finite element method and continuous H^1 -conforming finite elements. Both the Tikhonov regularization and conformity are also necessary to ensure convergence of discrete solutions with respect to the mesh size $h \rightarrow 0$. A detailed convergence analysis for a similar, but simpler semilinear optimal control problem for finite element discretizations was considered in [19].

1.2 Outline

The outline of the article is as follows: In Section 2, we derive our state equation which couples the control variable α to the resulting deformation u . We start from multiscale theory of scale separation and derive the constitutive equations on the macrolevel. Furthermore, we analyze the dependence of the stiffness tensor $A(x)$ on the local fiber orientation $\alpha(x)$ and show how to calculate it efficiently using coordinate transformation formulas. The optimal control problem is introduced in Section 3. We prove the existence of a global minimum and derive the necessary optimality condition as well as the KKT system. In Section 4, we formulate our adjoint-based gradient-type algorithm. Finally, Section 5 is devoted to the presentation of a prototypical numerical example to underline the capability of our method. We study its stability and convergence with respect to different regularization parameters κ and different meshes Ω_h .

2 Local Upscaling

In this section, we derive the state equation from multiscale theory. We refer to [25] or [10] for details on upscaling of the linear elasticity equation. Let $\varepsilon \ll 1$ be the ratio between micro and macro scale. The linear elasticity equation under consideration reads

$$\begin{aligned} -\operatorname{div}(A^\varepsilon \nabla u^\varepsilon) &= f \quad \text{in } \Omega, \\ u^\varepsilon &= u^d \quad \text{on } \Gamma, \\ (A^\varepsilon \nabla u^\varepsilon)n &= g \quad \text{on } \Gamma_N = \partial\Omega \setminus \Gamma. \end{aligned}$$

Here, $\Omega \subset \mathbb{R}^3$ is assumed to be sufficiently smooth and the Dirichlet part $\Gamma \subset \partial\Omega$ is of positive measure for each. The vector n denotes the outer unit normal along $\partial\Omega$. To ensure the unique solvability of the state equation, we assume the following conditions on $A^\varepsilon = (a_{ijkl}^\varepsilon)_{1 \leq i, j, k, l \leq 3}$

almost everywhere with positive constants ν and γ and the Frobenius matrix norm $\|\cdot\|_F$

$$a_{ijkl}^\varepsilon \in L^\infty(\Omega) \quad \text{for all } 1 \leq i, j, k, l \leq 3 \quad (1a)$$

$$a_{ijkl}^\varepsilon = a_{jikl}^\varepsilon = a_{klij}^\varepsilon \quad \text{for all } 1 \leq i, j, k, l \leq 3 \quad (1b)$$

$$a_{ijkl}^\varepsilon m_{ij} m_{kl} \geq \nu \|m\|_F^2 \quad \text{for any symmetric matrix } m \quad (1c)$$

$$\|A^\varepsilon m\|_F \leq \gamma \|m\|_F. \quad (1d)$$

It is well-known from multiscale theory^[10] that for ε sufficiently small, an approximation to u^ε can be calculated by solving the homogenized macroscale problem

$$\begin{aligned} -\operatorname{div}(A^0 \nabla u^0) &= f & \text{in } \Omega, \\ u^0 &= u^d & \text{on } \Gamma, \\ (A^0 \nabla u^0) n &= g & \text{on } \Gamma_N. \end{aligned}$$

The homogenized tensor A^0 is given by the solution of six microscale problems in every macroscopic point^[10].

Remark 2.1. *As we are only interested in the macroscopic part of the deformation u^ε , the approximation u^0 is sufficiently accurate for our purposes. It has been shown that properties (1) also hold for the effective tensor A^0 (cf. ^[10]).*

Here, we consider a unidirectional fiber orientation in every macroscopic point $x \in \Omega$, but which may vary locally over Ω . The effective tensor $A^0(x)$ only depends on the local fiber orientation $\alpha(x)$. We denote the operator that maps the fiber orientation function $\alpha(x)$ to the effective tensor $A^0(x)$ by

$$A : \mathcal{Q} \rightarrow (L^\infty(\Omega))^{3 \times 3 \times 3 \times 3}.$$

Using this notation the state equation reads

$$\begin{aligned} -\operatorname{div}(A(\alpha) \nabla u) &= f & \text{in } \Omega, \\ u &= u^d & \text{on } \Gamma, \\ (A(\alpha) \nabla u) n &= g & \text{on } \Gamma_N. \end{aligned}$$

Its weak formulation is given by:

Find $u \in u^d + H_0^1(\Omega; \Gamma)$, such that

$$(A(\alpha) \nabla u, \nabla \varphi) = (f, \varphi) - (g, \varphi)_{\Gamma_N} \quad \text{for all } \varphi \in H_0^1(\Omega; \Gamma). \quad (2)$$

where $H_0^1(\Omega; \Gamma)$ denotes the space of H^1 -functions with zero trace along Γ and u^d denotes an appropriate extension of the boundary data.

Proposition 2.2 (Meyers^[21]). *Assume that Ω convex or that $\partial\Omega \in C^{1,1}$ as well as $f \in L^2(\Omega)$, $g \in H^{1/2}(\Gamma_N)$ and u^d is the trace of a $W^{1,p}(\Omega)$ function \tilde{u}^d . Then, (2) has a unique solution in $W^{1,p}(\Omega)$ for $p \leq 6$ for every tensor $A(\alpha)$ fulfilling (1) and it holds for some constant $C > 0$*

$$\|u\|_{W^{1,p}} \leq C (\|f\|_{L^2} + \|g\|_{H^{1/2}(\Gamma_N)} + \|\tilde{u}^d\|_{W^{1,p}}). \quad (3)$$

2.1 The Effective Stiffness Tensor

Next, we want to study the relation $\alpha \rightarrow A(\alpha)$ which is essential for our optimization algorithm in detail.

Suppose, the effective stiffness tensor $A^0(0) = (a_{ijkl}^0(0))$, which corresponds to a fiber-matrix configuration with fibers oriented parallel to the x-axis, is given. We can calculate the effective tensor for the configuration that differs by an angle α in the x-y-plane by a simple coordinate transformation. Two-dimensional rotations in the x-y-plane can be described by the matrix $Q(\alpha) \in \mathbb{R}^{3 \times 3}$ with

$$Q(\alpha) = \begin{pmatrix} \cos(\alpha) & -\sin(\alpha) & 0 \\ \sin(\alpha) & \cos(\alpha) & 0 \\ 0 & 0 & 1 \end{pmatrix}.$$

Denoting its entries by q_{ij} , the fourth-order tensor $A(\alpha) = (a_{ijkl}(\alpha))$ transforms in the following way

$$a_{ijkl}(\alpha) = \sum_{1 \leq m, n, o, p \leq 3} q_{im}(\alpha) q_{jn}(\alpha) q_{ko}(\alpha) q_{lp}(\alpha) a_{mnop}^0(0). \quad (4)$$

Remark 2.3. *This coordinate transformation was already used by Beatty in^[6] and has been applied to find optimal stiffness tensors in a variety of works (cf. ^[24], ^[22]).*

Remark 2.4. *Note, that due to the periodicity of Q and (4) $A(\alpha)$ is π -periodic with respect to α . Furthermore, the coordinate transformation conserves properties (1) such that the state equation (2) is uniquely solvable for every $\alpha \in L^2(\Omega)$.*

For our optimization algorithm we will need the Frechét-derivative $\frac{d}{d\alpha}A(\alpha)$. We have to analyze the mappings

$$\alpha \mapsto (\sin(\alpha), \cos(\alpha)) \mapsto Q(\alpha) \mapsto A(\alpha).$$

Typical choices for the control space \mathcal{Q} like $L^2(\Omega)$ or $H^1(\Omega)$ are not feasible, as the operators $\sin(\alpha)$ and $\cos(\alpha)$ are neither differentiable from $L^2(\Omega)$ nor from $H^1(\Omega)$ into $L^\infty(\Omega)$ (see^[4]). On the other hand Frechét differentiability is given from $L^\infty(\Omega)$ into $L^\infty(\Omega)$. We will comment on the choice of the set of controls in the following section. For the sine operator the derivative in the direction $\delta\alpha \in L^\infty(\Omega)$ is given by

$$\sin'(\alpha)(\delta\alpha) = \cos(\alpha)\delta\alpha.$$

For the cosine operator we have analogously

$$\cos'(\alpha)(\delta\alpha) = -\sin(\alpha)\delta\alpha.$$

The derivatives of Q and A with respect to α read

$$Q'(\alpha)(\delta\alpha) = \begin{pmatrix} -\sin(\alpha)\delta\alpha & -\cos(\alpha)\delta\alpha & 0 \\ \cos(\alpha)\delta\alpha & -\sin(\alpha)\delta\alpha & 0 \\ 0 & 0 & 0 \end{pmatrix},$$

$$A'(\alpha)(\delta\alpha) = (a'_{ijkl}(\alpha))_{1 \leq i, j, k, l \leq 3},$$

where

$$a'_{ijkl}(\alpha)(\delta\alpha) = \sum_{1 \leq m, n, o, p \leq 3} \tilde{q}_{ijklmnop}(\alpha) \delta\alpha a_{mnop}^0,$$

$$\tilde{q}_{ijklmnop} = q'_{im}(\alpha)q_{jn}(\alpha)q_{ko}(\alpha)q_{lp}(\alpha) + q_{im}(\alpha)q'_{jn}(\alpha)q_{ko}(\alpha)q_{lp}(\alpha) \\ + q_{im}(\alpha)q_{jn}(\alpha)q'_{ko}(\alpha)q_{lp}(\alpha) + q_{im}(\alpha)q_{jn}(\alpha)q_{ko}(\alpha)q'_{lp}(\alpha).$$

3 The Optimization Problem

We are now ready for a precise formulation of the optimization problem. Let $\mathcal{U} = u^d + H_0^1(\Omega; \Gamma)$ be the state space and \mathcal{Q}^{ad} a set of admissible controls. Then, the concise optimization problem reads

$$\min_{(\alpha, u) \in \mathcal{Q}^{\text{ad}} \times \mathcal{U}} J(\alpha, u) := J^u(u) + \frac{\kappa}{2} \|\alpha\|_{H^1}^2 \quad (5a)$$

$$\text{subject to } (A(\alpha)\nabla u, \nabla \varphi) = (f, \varphi) - (g, \varphi)_{\Gamma_N} \quad \text{for all } \varphi \in H_0^1(\Omega; \Gamma). \quad (5b)$$

In addition to the notation used above, we suppose $\kappa > 0$ is a constant and J^u a convex and continuous functional.

3.1 The Set of Controls

For the controls, we choose a subset of the Hilbert space $H^1(\Omega)$. There are three main reasons for this choice: First, as we will see in the next subsection, we will need $\mathcal{Q}^{\text{ad}} \subset H^1(\Omega)$ in order to show existence of a global minimizer. Second, due to the nonlinearity of the state equation, we cannot expect higher regularity for the optimal control $\bar{\alpha}$ if we use a subset of $L^2(\Omega)$ as ansatz space. Thus, convergence of a discrete solution towards $\bar{\alpha}$ could not be guaranteed as the grid size tends to zero. Third, due to technical limitations regarding the construction process it might be desirable from an application point of view that the optimal fiber orientation shows a certain smoothness. Nevertheless, we remark that according to the application under consideration different choices of functional spaces are possible.

To ensure $\alpha \in L^\infty(\Omega)$, one could think of imposing the pointwise constraints

$$\mathcal{Q}^{\text{ad}} = \left\{ \alpha \in H^1(\Omega) \mid 0 \leq \alpha(x) \leq \pi \text{ a.e. in } \Omega \right\}$$

as A is π -periodic with respect to $\alpha(x)$. However, using these artificial bounds may rule out configurations that have fiber orientations $\alpha = \pi - \varepsilon$ and $\alpha = \varepsilon$ in regions close to each other. The value $\alpha = \varepsilon$, however, corresponds to the same orientation as $\alpha = \pi + \varepsilon$ and from a practical point of view no smoothness requirement is violated. Hence, it would be quite unnatural not to allow this configuration.

To fix this problem, we use the set of admissible controls

$$\mathcal{Q}^{\text{ad}} = \left\{ \alpha \in H^1(\Omega) \mid -c\pi \leq \alpha(x) \leq c\pi \text{ a.e. in } \Omega \right\}$$

for c sufficiently large.

3.2 Existence of a Solution

Next, we show the existence of a solution to Problem (5).

Lemma 3.1. *Let Ω be convex or $\partial\Omega \in C^{1,1}$ as well as $f \in L^2(\Omega)$, $g \in L^2(\Gamma_N)$ and u^d is the trace of a $W^{1,6}$ function. Furthermore, let $A(0)$ fulfill (1), $\kappa > 0$ and let J^u be a convex and continuous functional which is bounded from below. Then, problem (5) has at least one optimal solution $(\bar{\alpha}, \bar{u}) \in \mathcal{Q}^{\text{ad}} \times U$.*

Proof. We will follow the lines of the standard minimal sequence argument (cf. [35], [16]). Let

$$W^{\text{ad}} = \left\{ (\alpha, u) \in \mathcal{Q}^{\text{ad}} \times \mathcal{U} \mid (5b) \text{ holds} \right\},$$

$$\bar{j} = \inf_{(\alpha, u) \in W^{\text{ad}}} J(\alpha, u) > -\infty$$

and $(\alpha_k, u_k) \subset W^{\text{ad}}$ a minimal sequence, i.e.,

$$J(\alpha_k, u_k) \rightarrow \bar{j} \quad \text{for } k \rightarrow \infty.$$

Due to (3) u_k is bounded in $W^{1,6}(\Omega)$ and we can extract a subsequence of (α_k, u_k) such that u_k converges weakly to \bar{u} in $W^{1,6}(\Omega)$. Because of the compact embedding $H^1(\Omega) \subset L^5(\Omega)$, we can extract another subsequence such that α_k converges weakly in $H^1(\Omega)$ and strongly in $L^5(\Omega)$ to $\bar{\alpha}$. As \mathcal{Q}^{ad} is convex and closed, it is also weakly closed, and it holds $\bar{\alpha} \in \mathcal{Q}^{\text{ad}}$. Due to the Lipschitz continuity of the sine and cosine function and their products it follows, for $l = 0, \dots, 4$,

$$\left\| \sin^l(\alpha_k) \cos^{4-l}(\alpha_k) - \sin^l(\bar{\alpha}) \cos^{4-l}(\bar{\alpha}) \right\|_{L^5} \leq C \|\alpha_k - \bar{\alpha}\|_{L^5}$$

(cf. ^[35]) and thus $A(\alpha_k) \rightarrow A(\bar{\alpha})$ in $L^5(\Omega)$. These convergences are by far sufficient to deduce

$$(A(\alpha_k) \nabla u_k, \nabla \varphi) \rightarrow (A(\bar{\alpha}) \nabla \bar{u}, \nabla \varphi) \quad \text{for } k \rightarrow \infty$$

and thus $(\bar{\alpha}, \bar{u}) \in \mathcal{W}^{\text{ad}}$. The optimality of $(\bar{\alpha}, \bar{u})$ now follows by the lower semicontinuity of J . \square

3.3 Necessary Optimality Conditions

For every $\alpha \in \mathcal{Q}^{\text{ad}}$, we denote the unique solution u of the state equation by $u(\alpha)$. Using this notation, we define the so called reduced cost functional by

$$j(\alpha) = J(\alpha, u(\alpha)).$$

The necessary optimality condition for a local minimum α reads

$$j'(\alpha)(\delta \alpha - \alpha) \geq 0 \quad \text{for all } \delta \alpha \in \mathcal{Q}^{\text{ad}}. \quad (6)$$

To calculate the functional derivative $u'(\alpha)$, we use the implicit function theorem. Let

$$E(\alpha, u)(\varphi) := (A(\alpha) \nabla u, \nabla \varphi) - (f, \varphi) + (g, \varphi)_{\Gamma_N}.$$

The implicit function theorem ensures us the existence of the Frechét-derivative $\delta u := u'(\alpha)(\delta \alpha)$ given the differentiability of E with respect to both arguments and the boundedness of E_u . Under these assumptions $\delta u \in H_0^1(\Omega; \Gamma)$ solves

$$E_u(\alpha, u(\alpha))(\delta u(\alpha)) = -E_\alpha(\alpha, u(\alpha)),$$

i.e.,

$$(A(\alpha) \nabla \delta u, \nabla \varphi) = -(A'(\alpha)(\delta \alpha) \nabla \varphi, \nabla u(\alpha)) \quad \forall \varphi \in H_0^1(\Omega; \Gamma). \quad (7)$$

We define the adjoint variable $\lambda(\alpha) \in H_0^1(\Omega; \Gamma)$ as the solution of

$$(A(\alpha) \nabla \lambda(\alpha), \nabla \varphi) = - \left(\frac{d}{du} J^u(u(\alpha)), \varphi \right) \quad \text{for all } \varphi \in H_0^1(\Omega; \Gamma).$$

Now, we can rewrite j' in the following way

$$\begin{aligned} j'(\alpha)(\delta \alpha) &= \left(\frac{d}{du} J^u(u(\alpha)), \delta u(\alpha) \right) + \kappa(\alpha, \delta \alpha) + \kappa(\nabla \alpha, \nabla \delta \alpha) \\ &= -(A(\alpha) \nabla \lambda(\alpha), \nabla \delta u(\alpha)) + \kappa(\alpha, \delta \alpha) + \kappa(\nabla \alpha, \nabla \delta \alpha) \\ &= (A'(\alpha)(\delta \alpha) \nabla \lambda(\alpha), \nabla u(\alpha)) + \kappa(\alpha, \delta \alpha) + \kappa(\nabla \alpha, \nabla \delta \alpha). \end{aligned} \quad (8)$$

Summarizing, we get the following KKT-system for an optimal control α of (5) and its corresponding optimal state $u(\alpha) \in u^d + H_0^1(\Omega; \Gamma)$ and adjoint state $\lambda(\alpha) \in H_0^1(\Omega; \Gamma)$:

$$\begin{aligned} (A(\alpha)\nabla u, \nabla\varphi) &= (f, \varphi) - (g, \varphi)_{\Gamma_N} \quad \text{for all } \varphi \in H_0^1(\Omega; \Gamma) \\ (A(\alpha)\nabla\lambda(\alpha), \nabla\varphi) &= - \left(\frac{d}{du} J^u(u(\alpha)), \varphi \right) \quad \text{for all } \varphi \in H_0^1(\Omega; \Gamma) \\ (A'(\alpha)(\delta\alpha - \alpha)\nabla\lambda(\alpha), \nabla u(\alpha)) &+ \kappa(\alpha, \delta\alpha - \alpha) \\ &+ \kappa(\nabla\alpha, \nabla(\delta\alpha - \alpha)) \geq 0 \quad \text{for all } \delta\alpha \in \mathcal{Q}^{ad}. \end{aligned}$$

4 The Gradient Algorithm

The derivative information derived so far is sufficient to design a steepest descent algorithm for the solution of the minimization problem under consideration.

In particular, we propose the following adjoint based gradient-type algorithm:

1. Calculate the effective stiffness tensor $A^0(0)$ by numerical upscaling (see Chapter 2) and choose $\alpha^0 \in \mathcal{Q}^{ad}$.

For $k=0,1,\dots$:

2. Calculate $u^k \in u^d + H_0^1(\Omega; \Gamma)$ solving the state equation

$$(A(\alpha^k)\nabla u^k, \nabla\varphi) = (f, \varphi) - (g, \varphi)_{\Gamma_N} \quad \forall \varphi \in H_0^1(\Omega; \Gamma).$$

3. Calculate $\lambda^k \in H_0^1(\Omega; \Gamma)$ as solution of the adjoint equation

$$(A(\alpha^k)\nabla\lambda^k, \nabla\varphi) = - \left(\frac{d}{du} J^u(u^k), \varphi \right) \quad \forall \varphi \in H_0^1(\Omega; \Gamma).$$

4. Calculate the Riesz representation g^k of the gradient $j'(\alpha^k)(\delta\alpha)$ in $H^1(\Omega)$ by solving

$$(\nabla g^k, \nabla\delta\alpha) + (g^k, \delta\alpha) = j'(\alpha^k)(\delta\alpha) \quad \forall \delta\alpha \in H^1(\Omega),$$

where

$$j'(\alpha^k)(\delta\alpha) = (A'(\alpha)(\delta\alpha)\nabla\lambda(\alpha), \nabla u(\alpha)) + \kappa(\alpha, \delta\alpha) + \kappa(\nabla\alpha, \nabla\delta\alpha).$$

5. Set $s^k = \frac{g^k}{\|g^k\|_{H^1}}$, choose a step size σ^k and set

$$\alpha^{k+1} = P_{\mathcal{Q}^{ad}}(\alpha^k - \sigma^k s^k),$$

where $P_{\mathcal{Q}^{ad}}$ denotes the projection onto \mathcal{Q}^{ad} .

Remark 4.1. Of course, instead of the gradient type algorithm proposed, a higher-order accurate scheme, e.g., a Newton-type algorithm in combination with an active set strategy can be used (cf. [16] for different possibilities).

Remark 4.2. Note, that in step 2 to 4, we need the stiffness tensor $A(\alpha)(x)$ and its derivative $A'(\alpha)(x)$ in every Gaussian point x of the mesh. These tensors are calculated according to section 2.1 by the coordinate transformation formulas for rotation of $\alpha(x)$. In this way the costly subsequent solution of microlevel problems is avoided.

Remark 4.3. To find an appropriate step size in step 5 we use the projected Armijo rule^[5,16]. We choose the maximal $\sigma^k \in \{1, \frac{1}{2}, \frac{1}{4}, \dots\}$ such that

$$j(P_{\mathcal{Q}^{ad}}(\alpha^k - \sigma^k s^k)) - j(\alpha^k) \leq -\frac{\gamma}{\sigma^k} \|P_{\mathcal{Q}^{ad}}(\alpha^k - \sigma^k s^k) - \alpha^k\|_{H^1}$$

holds.

Remark 4.4. As the relationship $\alpha \rightarrow u(\alpha)$ is highly nonlinear, j defines in general a nonconvex functional on $H^1(\Omega)$, even if J^u is convex. I.e., standard optimization algorithms will in general only converge to a local minimum. In order to find a minimum with good properties from a global point of view, we calculate the functional value of several reference configurations in advance and take the best configuration as a starting value. Furthermore, in practical applications a good initial guess might often be available. For more involved strategies in order to find global minima we refer to^[17]. Here, we are only seeking local minima.

Remark 4.5. The algorithm requires in step 2 to 4 the solution of 2 linear systems of linear elasticity type and one system of scalar elliptic type in every iteration. Furthermore, using the Armijo rule, we have to calculate $u(\alpha)$ for several candidates α , which requires to solve the state equation once for every candidate. Hence, typically we end up by solving 3 to 6 systems of linear ellipticity type and one of scalar elliptic type in each iteration. In comparison to solving several microproblems in every iteration the computational cost per iteration is very low. As stopping criterion, we choose

$$\frac{\|\alpha^k - P_{\mathcal{Q}^{ad}}(\alpha^k - \sigma^k s^k)\|_{H^1}}{\|\alpha^0 - P_{\mathcal{Q}^{ad}}(\alpha^0 - \sigma^0 s^0)\|_{H^1}} \leq TOL$$

where g^k stands again for the Riesz representation of the gradient of j .

Remark 4.6. In our numerical tests the choice of $c=2$ in \mathcal{Q}^{ad} was sufficient to ensure that both bounds were not becoming active.

5 Numerical Examples

In this section, we study a prototypical numerical example in order to demonstrate the capabilities of our algorithm. Our objective is to design a material which shows minimal deformation in x -direction under a given stretching in y -direction.

5.1 Model problem

As a model problem, we want to optimize the fiber orientation in a structure consisting of a cube containing a cylindrical hole in the middle

$$\Omega^c = \left\{ (x, y, z) \in \mathbb{R}^3 \mid -10 < x, y < 10, 0 < z < 10, \sqrt{(x^2 + y^2)} > 4 \right\}.$$

We set the volume force $f = 0$ and prescribe the displacement of the boundary on the lower face and upper face of the cube (cf. Figure 1, left side). Furthermore, we impose zero displacement in normal direction on the frontface and backface. As mentioned above, we are interested in the displacement in x -direction u_1 . Clearly, the indicated stretching will lead to a deformation u_1 towards the midplane $x = 0$. Due to symmetry reasons, it is sufficient to simulate a quarter of the structure (cf. Figure 1, right side).

$$\Omega = \left\{ (x, y, z) \mid 0 < x, y, z < 10, \sqrt{(x^2 + y^2)} > 4 \right\}.$$

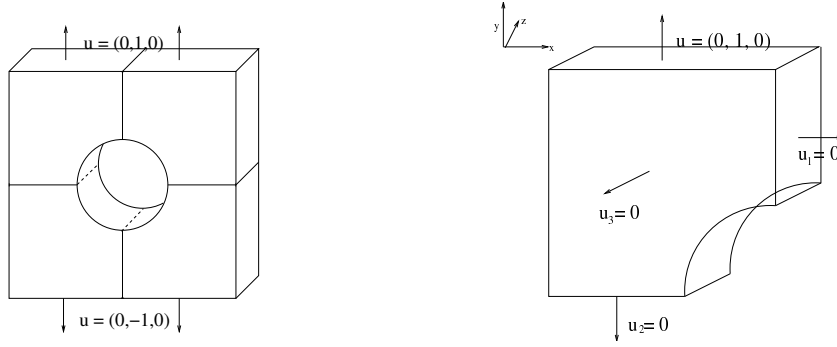


Figure 1. Model problem

We impose the following Dirichlet boundary conditions $u^d = (u_1^d, u_2^d, u_3^d)$

$$u^d = (0, 1, 0) \text{ on } \Gamma_{\text{top}},$$

$$u_2^d = 0 \text{ on } \Gamma_{\text{left}},$$

$$u_3^d = 0 \text{ on } \Gamma_{\text{front}} \cup \Gamma_{\text{back}}.$$

with the intuitive notation for top, front, back and left boundary.

We want to design an optimal material which shows minimal deformation in x-direction under this load, i.e.,

$$\begin{aligned} \min_{(\alpha, u) \in \mathcal{Q}^{\text{ad}} \times \mathcal{U}} J(\alpha, u) &:= \frac{1}{2} \|u_1\|_{L^2}^2 + \frac{\kappa}{2} \|\alpha\|_{H^1}^2 \\ \text{subject to } -\operatorname{div}(A(\alpha)\nabla u) &= 0 \quad \text{in } \Omega, \\ u_i &= u_i^d \quad \text{on } \Gamma_i \quad i = 1, 2, 3, \\ (A(\alpha)\nabla u \cdot n)_i &= 0 \quad \text{on } \partial\Omega \setminus \Gamma_i \quad i = 1, 2, 3, \end{aligned}$$

where

$$\Gamma_1 = \Gamma_{\text{top}}, \Gamma_2 = \Gamma_{\text{left}} \cup \Gamma_{\text{top}}, \Gamma_3 = \Gamma_{\text{top}} \cup \Gamma_{\text{front}} \cup \Gamma_{\text{back}}.$$

As material parameters we choose the Young's modulus E and Poisson's ratio ν for fiber and matrix material by

$$E^{\text{mat}} = 0.3, \quad \nu^{\text{mat}} = 0.2 \quad E^{\text{fib}} = 100, \quad \nu^{\text{fib}} = 0.3.$$

On the microscale we assume Hooke's law for the fiber and matrix material, respectively, which reads in matrix notation

$$\begin{pmatrix} \sigma_{11} \\ \sigma_{22} \\ \sigma_{33} \\ \sigma_{23} \\ \sigma_{13} \\ \sigma_{12} \end{pmatrix} = \frac{E}{(1+\nu)(1-2\nu)} \begin{pmatrix} 1-\nu & \nu & \nu & 0 & 0 & 0 \\ \nu & 1-\nu & \nu & 0 & 0 & 0 \\ \nu & \nu & 1-\nu & 0 & 0 & 0 \\ 0 & 0 & 0 & \frac{1-2\nu}{2} & 0 & 0 \\ 0 & 0 & 0 & 0 & \frac{1-2\nu}{2} & 0 \\ 0 & 0 & 0 & 0 & 0 & \frac{1-2\nu}{2} \end{pmatrix} \begin{pmatrix} e_{11} \\ e_{22} \\ e_{33} \\ 2e_{23} \\ 2e_{13} \\ 2e_{12} \end{pmatrix}.$$

According to Section 2 we calculate the effective tensor $A^0(0)$ for fibers parallel to the x-axis by solving six cell problems in a reference structure Y . For the generation of the microstructure geometry, we use the software *GeoDict*^[14] where we impose a fiber-volume fraction of 5%. The microstructure obtained using *GeoDict* is shown in Figure 2.



Figure 2. Microstructure for calculating $A^0(0)$

5.2 Discretization

Let \mathcal{T}_h be a family of quasiuniform triangulations of Ω into closed tetrahedrons $T_i, i = 1 \dots N$. \mathcal{P}_1 the space of H^1 -conforming P_1 finite elements on this triangulation. We define the discrete state space by

$$\mathcal{U}_h = \mathcal{U} \cap (\mathcal{P}_1)^3.$$

For the discretization of the control space we set

$$\mathcal{Q}_h^{\text{ad}} = P_1 \cap \mathcal{Q}^{\text{ad}}.$$

5.3 Results

In order to find a good initial value α^0 and to be able to compare the obtained optimal solution, we calculated the functional

$$J^u(u(\alpha)) = \frac{1}{2} \|u_1(\alpha)\|_{L^2}^2$$

for different constant fiber orientations α_i and the corresponding deformations $u(\alpha_i)$ in advance. After calculating $A^0(0)$ we obtain the remaining tensors again using the transformation formulas given in chapter 2.1. We realized calculations for

$$\alpha_k \equiv \frac{5k\pi}{180}, \quad k = 0, \dots, 35.$$

For our simulations we used the finite element software *FeelMath* (*Finite Elements for elastic Materials and Homogenization*^[12]), which has been developed at the Fraunhofer Institute for Industrial Mathematics. The results are shown in Figure 3. For further comparison, we also calculated J^u for a random fiber distribution and for a pure matrix material without fibers and plotted the respective values as constant dashed lines. As we can see, we get the lowest value for a fiber orientation of 115 degrees ($k = 23$). Thus, we choose $\alpha^0 = \alpha_{23} \equiv \frac{115\pi}{180}$ as initial control function.

For our optimization algorithm, we set $\kappa = 10^{-5}$ and use a mesh of nearly constant cell size $h = 0.5$ inside the domain, while we impose a cell size of $h = 0.2$ near critical boundaries. The mesh is shown in Figure 4. The dependence of the algorithms's convergence on the regularization parameter and mesh will be analyzed in the next subsections.

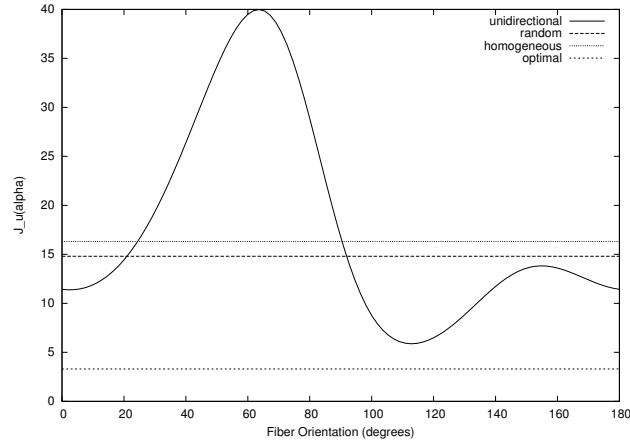


Figure 3. Values of the objective functional for different constant fiber orientations, random oriented fibers, a homogeneous material without fibers and the optimal orientation found using the algorithm given in section 4

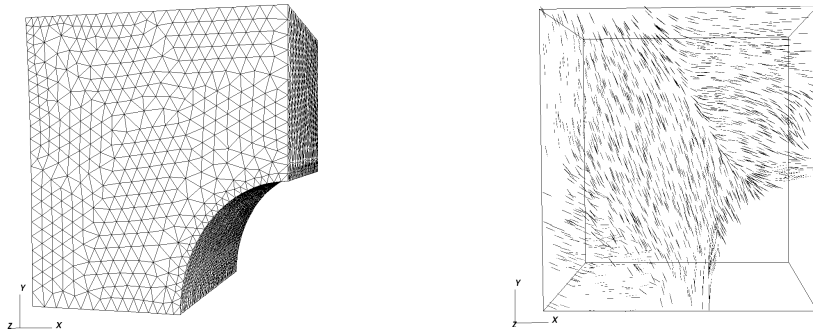


Figure 4. Used mesh (left) and the optimal fiber orientation (right)

While the lowest value we get for constant fiber orientation was $J^u(u(\alpha_{23})) = 5.939$, our optimization algorithm converges to $\bar{\alpha}$ with $J^u(u(\bar{\alpha})) = 3.310$. Thus, we were able to reduce the deformation in x-direction by 44,3% in comparison to the best constant fiber orientation. For comparison, we have included the value of the objective functional for the optimal configuration as another dashed line in Figure 4. The optimal fiber orientation $\bar{\alpha}$ is illustrated in Figure 4 on the right. We can see that in regions near the right and the lower boundary, a larger angle than 115 degrees is favorable while in the middle of the domain the optimal fiber orientation we found shows an angle smaller than the starting value of 115 degrees. As we chose a rather small regularization parameter κ fiber orientations change quite quickly between different regions. Nevertheless, we observe a sufficiently smooth behaviour of α for practical purposes. Increasing κ leads to a bigger influence of the H^1 -Tikhonov regularization and a slower variation of fiber angles.

5.4 Regularization Parameter Studies

To study the dependence of our algorithm on the regularization parameter κ , we realized calculations for $\kappa = 10^{-3}$, 10^{-4} , and 10^{-5} on the mesh introduced in the last section. As initial value we used $\alpha \equiv \frac{\pi}{2}$ and as stopping criterion, we imposed a reduction factor of $\text{TOL} = 10^{-2}$ for the H^1 -norm of the reduced gradient. The results are shown in Figure 5. Figure 5 (a) shows the

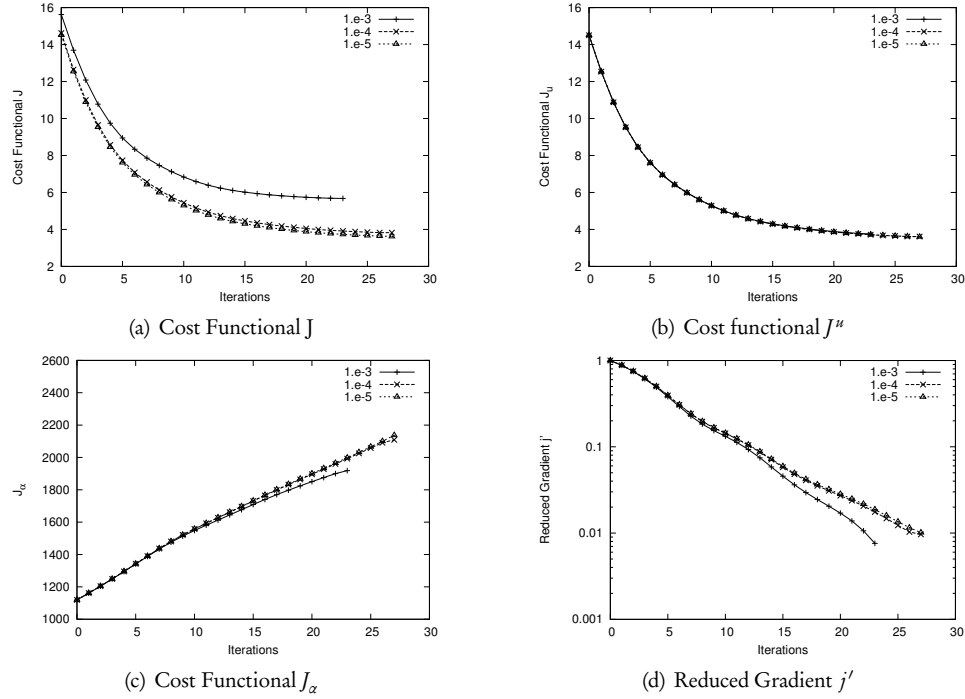


Figure 5. Influence of the regularization parameter κ

convergence behaviour of the cost functional

$$J(u, \alpha) = J''(u(\alpha)) + J_\alpha(\alpha) = \frac{1}{2} \|u_1\|^2 + \frac{\kappa}{2} \|\alpha\|_{H^1}^2.$$

Clearly, a bigger regularization parameter leads to a bigger value in the objective functional as the regularization part increases. Figure 5 (b) shows the value of the deformation part

$$J''(u(\alpha)) = \frac{1}{2} \|u_1(\alpha)\|^2.$$

We get a slightly larger deformation for bigger values of κ . This is because κ is the weight of the regularization part and thus, a bigger κ makes smaller and smoother angle distributions more favourable. In Figure 5 (c) we plot the behaviour of the penalty part

$$J_\alpha(\alpha) = \frac{1}{2} \|\alpha\|_{H^1}^2.$$

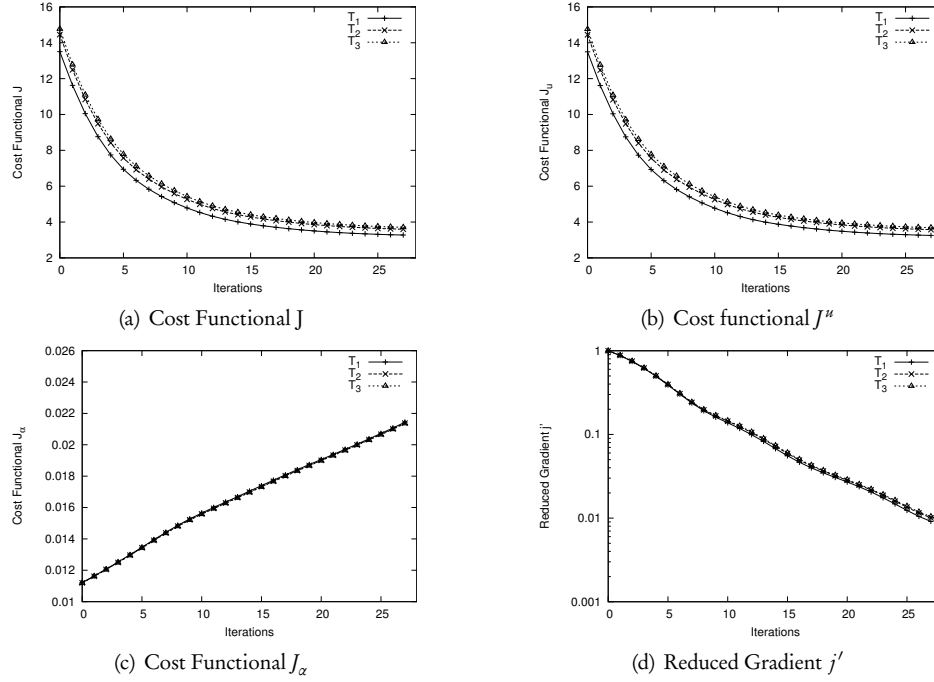
As one would expect, the bigger the regularization parameter κ , the smaller gets $\|\alpha\|_{H^1}$. Finally, in 5 (d) we plotted the behaviour of the reduced gradient. We observe that the bigger the regularization parameter the faster the decrease of the reduced gradient and hence less iterations are required. Clearly, this is also what we had expected. The initial reduced gradient is reduced by a two orders of magnitude after 23 to 27 iterations.

5.5 Dependence on the Mesh

In this section, we fix the regularization parameter to $\kappa = 10^{-5}$ and analyze the convergence behaviour on different meshes. Therefore, we realized calculations on meshes with nearly constant

Table 1. Discretization

Triangulation	Cell size	Number of Elements
\mathcal{T}_1	1	8768
\mathcal{T}_2	0.5	69284
\mathcal{T}_3	0.25	553145

Figure 6. Convergence behaviour on different meshes T_i

cell size $h_1 = 1$, $h_2 = 0.5$ and $h_3 = 0.25$. The number of elements and cell sizes are summarized in Table 1. In Figure 6(a-c), we plot the decrease of the objective functional $J(u(\alpha), \alpha)$ and its components $J''(u(\alpha))$ and $J_\alpha(\alpha)$. We notice a similar convergence behaviour on all meshes. In Figure 6(a) and (b), we see that the functional values on finer grids are slightly larger than those on coarser grids. The deviation lies within the range of the discretization error, however and is much smaller on the finer meshes. Finally, in Figure 6(d) we see that the decrease of the reduced gradient shows a very similar behaviour on all meshes. Thus, we have shown that our algorithm is almost independent with respect to grid size and mesh.

6 Conclusions

We presented an efficient algorithm to find an optimal fiber orientation in composite materials. Fiber orientation is regarded as a function of space on the macrolevel which allows for a big class of different fiber orientation distributions and does not restrict orientation to be constant within, e.g., a given layer. The approach is proposed within a function space setting which makes the imposition of smoothness requirements straightforward and allows for rather general objective functionals. In order to guarantee its well-posedness we use a Tikhonov regularization term.

The algorithm we proposed is a one level optimization algorithm which optimizes with respect

to the fiber orientation directly. The costly solve of a big number of microlevel problems is avoided using coordinate transformation formulas. Therefore, it is sufficient to do one microlevel calculation in advance. We used an adjoint-based gradient type algorithm, but generalization to higher-order schemes is straightforward. The algorithm was tested for a prototypical example and showed good behaviour with respect to mesh independence and regularization parameter studies. Furthermore, the framework we developed is clearly not restricted to linearized elasticity. Other applications where anisotropy plays an important role can be treated in an analogous way. As an example consider for example the design of an optimal porous media for filter applications.

Within the context of composite materials, optimization with respect to local fiber volume fraction (FVF) might be treated in a similar way. For simultaneous material optimization, we propose a combination of the presented approach with the Discrete Material Optimization Method (DMO, ^[31], ^[32]).

Acknowledgment

The present work was funded by the Stiftung Rheinland-Pfalz für Innovation within the project "Multiskalensimulation für die Entwicklung von Hochleistungsverbundwerkstoffen (MUSSEH)" at Fraunhofer Institute for Industrial Mathematics. The third author was supported by the DFG via SPP 1253.

References

- [1] R.D. Adams and D.G.C. Bacon. Effect of fiber orientation and laminate geometry on the dynamic properties of cfrp. *J. Comp. Mat.*, 7(4):402–428, 1973.
- [2] Gregoire Allaire. *Shape Optimization by the Homogenization Method*. Springer, Berlin – Heidelberg – New York, 2001. ISBN 0-387-95298-5.
- [3] Grégoire Allaire, Eric Bonnetier, Gilles Francfort, and Francois Jouve. Shape optimization by the homogenization method. *Num. Math.*, 76:27–68, 1997. ISSN 0029-599X. doi: 10.1007/s002110050253.
- [4] Jürgen Appell and Petr P. Zabrejko. *Nonlinear Superposition Operators*. Cambridge Tracts in Mathematics. Cambridge University Press, 1990. ISBN 0-521-36102-8.
- [5] Larry Armijo. Minimization of functions having lipschitz continuous first partial derivatives. *Pacific J. Math.*, 16(1):1–3, 1966.
- [6] Millard F Beatty. Kinematics of finite rigid body displacements. *Ann.J.Phys.*, 34:949–956, 1966.
- [7] Martin P. Bendsøe. *Optimization of Structural Topology, Shape and Material*. Springer, Berlin – Heidelberg – New York, 1995. ISBN 3-540-59057-9.
- [8] Martin P. Bendsøe and Noboru Kikuchi. Generating optimal topologies in structural design using a homogenization method. *Comp. Methods Appl. Mech. Engrg.*, 71:197–224, 1988.
- [9] R. M. Christensen. *Mechanics of composite materials*. Wiley, 1979.
- [10] Doina Cioranescu and Patrizia Donato. *An Introduction to Homogenization*. Oxford Lecture Series in Mathematics and its applications. Oxford University Press, 1999. ISBN 0-19-856554-2.

- [11] A. Díaz and R. Lipton. Optimal material layout for 3d elastic structures. *Structural Optimization*, 13:60–64, 1997.
- [12] FeelMath. FeelMath: Finite elements for elastic materials and homogenization. developed at Fraunhofer Institute for Industrial Mathematics.
- [13] Benedict Geihe, Martin Lenz, Martin Rumpf, and Rüdiger Schultz. Risk averse elastic shape optimization with parametrized fine scale geometry. *Math. Program.*, pages 1–21, 2012. ISSN 0025-5610. doi: 10.1007/s10107-012-0531-1.
- [14] GeoDict. GeoDict: Geometric material models and computational predictions of material properties. URL <http://www.geodict.com>. <http://www.geodict.com>, developed at Fraunhofer Institute for Industrial Mathematics.
- [15] Z. Hashin and S. Shtrikman. A variational approach to the theory of elastic behaviour of multiphase materials. *J. Mech. Phys. Solids*, 11:127–140, 1963.
- [16] Michael Hinze, Rene Pinnau, Michael Ulbrich, and Stefan Ulbrich. *Optimization with PDE Constraints*, volume 23 of *Mathematical Modelling: Theory and Applications*. Springer, Berlin – Heidelberg – New York, 2009. ISBN 978-1-4020-8838-4.
- [17] R. Horst, P. M. Pardalos, and N. V. Thoai. *Introduction to Global Optimization*. Kluwer Academic, 2000.
- [18] J.L. Kardos. Critical issues in achieving desirable mechanicproperties for short fiber composites. *Pure and Appl. Chem.*, 57(11):1651–1657, 1985.
- [19] Axel Kroener and Boris Vexler. A priori error estimates for elliptic optimal control problems with a bilinear state equation. *J. Comp. Appl. Math.*, 230(2):781–802, 2009.
- [20] Oliver Meyer. *Kurzfaser-Preform-Technologie zur kraftflussgerechten Herstellung von Faserverbundbauteilen*. PhD thesis, Universität Stuttgart, 2008.
- [21] Norman G. Meyers. An L^p -estimate for the gradient of solutions of second order elliptic divergence equations. *Annali della Scuola Normale Superiore di Pisa*, 17(3):189–206, 1963.
- [22] J.S Moita, J Infante Barbosa, C.A Mota Soares, and C.M Mota Soares. Sensitivity analysis and optimal design of geometrically non-linear laminated plates and shells. *Computers and Structures*, 76(1–3):407 – 420, 2000.
- [23] François Murat. Contre-exemples pour divers problèmes où le contrôle intervient dans les coefficients. *Ann. Mat. Pura. Appl.*, 112:49–68, 1977.
- [24] A.N. Norris. Optimal orientation of anisotropic solids. *Quart. J. Mech. Appl. Math.*, 59(1): 29–52, 2005.
- [25] O.A. Oleinik, A.S. Shamaev, and G.A. Yosifian. *Mathematical Problems in Elasticity and Homogenization*, volume 26 of *Studies in Mathematics and its Applications*. North-Holland, Amsterdam – London – New York – Tokyo, 1992.
- [26] G. Papanicolau, A. Bensoussan, and J.L. Lions. *Asymptotic Analysis for Periodic Structures*. Studies in Mathematics and its Applications. Elsevier Science, 1978.
- [27] P. Pedersen. On optimal orientation of orthotropic materials. *Struct. Multidiscip. Optim.*, 1: 101–106, 1989.
- [28] H. Rodrigues, J.M. Guedes, and M.P. Bendsøe. Hierarchical optimization of material and structure. *Struct. Multidiscip. Optim.*, 24:1–10, 2002.

- [29] G.A. Seregin and V.A. Troitskii. On the best position of elastic symmetry planes in an orthotropic body. *J. Appl. Math. Mech.*, 45:139–142, 1981.
- [30] S. Staub, H. Andrä, M. Kabel, and T. Zangmeister. Multi-scale simulation of viscoelastic fiber-reinforced composites. *Technische Mechanik*, 32(1):70–83, 2012.
- [31] J. Stegmann. *Analysis and Optimization of Laminated Composite Shell Structures*. Dissertation, Institute of Mechanical Engineering, Aalborg University, Denmark, 2005.
- [32] J. Stegmann and E. Lund. Discrete material optimization of general composite shell structures. *Int. J. Num. Meth. Engrg.*, 62(14):2009–2027, 2005.
- [33] S.A. Suarez, R.F. Gibson, C.T. Sun, and S.K. Chaturvedi. The influence of fiber length and fiber orientation on damping and stiffness of polymer composite materials. *Exp. Mech.*, 26: 175–184, 1986.
- [34] P.S. Theocaris and G.E. Stavroulakis. Optimal material design in composites: An iterative approach based on homogenized cells. *Comput. Methods Appl. Mech. Engrg.*, 169:31–42, 1999.
- [35] Fredi Tröltzsch. *Optimal Control of Partial Differential Equations: Theory, Methods and Applications*. Graduate studies in mathematics. American Mathematical Society, 2010.